

Distilling Functional Rearrangement Priors from Large Models

Yiming Zeng*, Mingdong Wu*, Long Yang, Jiyao Zhang, Hao Ding, Hui Cheng, Hao Dong

Abstract—Object rearrangement, a fundamental challenge in robotics, demands versatile strategies to handle diverse objects, configurations, and functional needs. To achieve this, the AI robot needs to learn functional rearrangement priors in order to specify precise goals that meet the functional requirements. Previous methods typically learn such priors from either laborious human annotations or manually designed heuristics, which limits scalability and generalization. In this work, we propose a novel approach that leverages large models to distill functional rearrangement priors. Specifically, our approach collects diverse arrangement examples using both LLMs and VLMs and then distills the examples into a diffusion model. During test time, the learned diffusion model is conditioned on the initial configuration and guides the positioning of objects to meet functional requirements. In this manner, we create a handshaking point that combines the strengths of conditional generative models and large models. Extensive experiments on multiple domains, including real-world scenarios, demonstrate the effectiveness of our approach in generating compatible goals for object rearrangement tasks, significantly outperforming baseline methods. Our real-world results can be seen on <https://sites.google.com/view/lvdiffusion>.

I. INTRODUCTION

Object rearrangement [1] is a fundamental challenge in robotics that is widely encountered in our daily lives, such as when organizing a cluttered writing desk, reconfiguring furniture in the bedroom, or setting up a dining table for a left-handed user. This task requires the AI robot to specify precise goals, including object locations, and then rearrange the objects to achieve those goals. To accomplish this, the AI robot needs to learn *functional rearrangement priors*, *i.e.*, how to position the objects to fulfill functional requirements. These priors should be capable of handling diverse objects, configurations, and functional needs. This presents a significant challenge for robotics, as manually designing a reward or goal function is difficult [2].

Previous works [3], [4], [5], [6], [2] typically learn such priors from a dataset either manually designed by humans or synthesized using heuristic rules. However, the former approach requires laborious human annotations, limiting its **scalability**. The latter approach depends on hard-coded heuristics, making it difficult to **generalize** to diverse configurations. On the other hand, DALL-E-Bot [7] proposes an alternative direction that leverages an internet-scale pre-trained diffusion model to generate the arrangement goal according to the initial state. However, this approach suffers from a significant

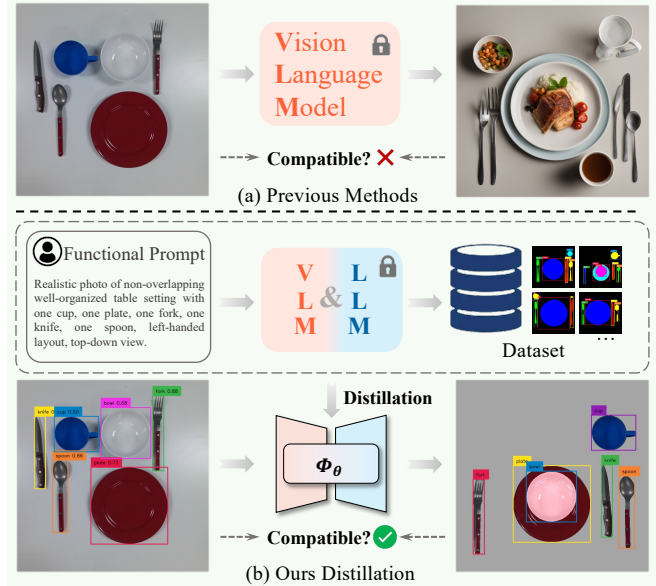


Fig. 1. (a): Integrating a large model into the rearrangement pipeline may lead to *compatibility issues*. (b): Differently, we *distill* a conditional generative model from the large models, which helps alleviate this issue.

compatibility issue: there is no guarantee that the generated goal will be **compatible** with the ground-truth configuration. Additionally, this method is time-consuming as it requires multiple inferences from a large model. In light of these, we pose the following question:

*How to learn **generalizable** functional rearrangement priors that can generate **compatible** goals for diverse configurations, in a **scalable** manner?*

As shown in Figure 7, our key idea is to distill functional rearrangement priors from large models into compact representations. Firstly, we prompt a large Visual-Language-Model (VLM), such as StableDiffusion [8], to generate a dataset filled with arrangement examples (*i.e.*, goals) that satisfy the functional needs. Then, we train a conditional generative model (*e.g.*, diffusion model [9]) on these arrangement examples to model the distilled functional rearrangement priors. In this manner, we create a handshaking point that combines the strengths of the conditional generative model and large models. On one hand, prompting large models allows us to collect arrangement examples across a wide range of diverse configurations, facilitating generalization in a scalable manner. On the other hand, distilling the gathered data into a conditional generative model enables us to generate feasible goals that are compatible with the initial conditions.

Unfortunately, as also observed by [10], [11], the output of the VLM cannot be guaranteed to be consistent with the prompt input, which may lead us to distill incorrect

* indicates equal contribution

Mingdong Wu, Jiyao Zhang, Long Yang and Hao Dong are with Hyperplane Lab, School of CS, Peking University and National Key Laboratory for Multimedia Information Processing. Yiming Zeng, Hao Ding, and Hui Cheng are with Sun Yat-Sen University. Jiyao Zhang is also with the Beijing Academy of Artificial Intelligence (BAAI).

Corresponding to hao.dong@pku.edu.cn and chengh9@mail.sysu.edu.cn

knowledge from large models. Specifically, the generated results may deviate from the specified number and types of objects in the prompt, and may not perfectly align with the functional requirements outlined in the prompt. For instance, when prompted with “a well-organized arrangement of a fork, two bowls, and a plate on a dinner table” the VLM may generate an arrangement with two randomly placed bowls (*i.e.*, *violating functional requirement*) multiple forks (*i.e.*, *different number*), and a mug (*i.e.*, *an unexpected object type*).

To alleviate this issue, we integrate a Large Language Model after prompting the VLM to assist in correcting the generated examples. We initially instruct the VLM with an original prompt, such as “Realistic photo of the non-overlapping, well-organized table setting with one cup, one plate, one fork, one knife, one spoon, left-handed layout, top-down”, and extract object states (*e.g.*, bounding boxes) through an off-the-shelf perception module (*e.g.*, DINO [12]). Afterward, we input these object states and prompt the Large Language Model (LLM) using a Chain-of-Thoughts approach [13] to fine-tune their positions in order to better align with the functional requirements.

We conduct experiments in multiple scenarios and functionalities to demonstrate the effectiveness of our approach in learning functional rearrangement priors and deploying them in real-world rearrangements. Extensive results and analysis showcase that our method significantly outperforms the baseline in generating compatible rearrangement goals for a large variety of configurations. Ablation studies further suggest that both LLM and VLM play indispensable roles in distilling the functional rearrangement priors.

In summary, our contributions are summarised as follows:

- We introduce a novel framework that trains a diffusion model to distill functional rearrangement priors from both LLM and VLM for object rearrangement.
- We propose leveraging the LLM, such as GPT4, to help alleviate the misalignment between the generated results and the VLM prompt.
- We conduct extensive experiments to demonstrate the effectiveness of our approach in generating compatible goals and real-world deployment.

II. RELATED WORK

A. Object Rearrangement with Functional Requirements

The object rearrangement is a fundamental challenge [1] and a long-studied problem [14], [15], [16] in robotics and the graphics community [17], [18], [19], [20], [21], [22]. One of the keys to tackling object rearrangement is goal specification, *i.e.*, how to specify precise rearrangement goals to meet the functional requirements. Early works typically focus on manually designing rules/ energy functions to find a goal [14], [15], [16] or synthesizing a scene configuration [18], [19], [20], [21] that satisfies the preference of the user.

Some recent works learn such priors by training a conditional generative model from a dataset either manually designed by humans or synthesized using heuristic rules. Neatnet [6] tries to learn a GNN from a human-collected

dataset to output an arrangement tailored to human preferences. TarGF [2] and LEGO-NET [22] learn gradient fields that provide guiding directions to rearrange objects, via Denoising-Score-Matching [23] from the indoor-scene dataset designed by artists. StructDiffusion [4], StructFormer [3] and RPDiff [5] learn a conditional generative model from arrangement examples generated in simulation using a handcrafted function. However, these methods either depend on hard-coded heuristics that make them difficult to generalize to diverse configurations or require laborious human annotations that limit the scalability.

Another stream of research attempts to leverage the Large Language Model (LLM) or large Visual Language Model (VLM) for goal specification. [24], [25] notice the necessity of automatic goal inference for tying rooms and exploit the commonsense knowledge from LLM or memex graph to infer rearrangements goals when the goal is unspecified. TidyBot [26] also leverages an LLM to summarize the rearrangement preference from a few examples provided by the user. However, it is difficult for LLM to specify the coordinate-level goal. The most recent work, DALL-E-Bot [7], integrates a large VLM, such as Dall-E 2 [27] to generate the arrangement goal according to the initial state. However, there is no guarantee that the generated goal will be compatible with the ground-truth configuration.

Differing from those studies, our approach leverages the LLM and VLM to collaboratively collect arrangement examples, enabling generalizable and scalable data collection, and distills them into a conditional generative model.

B. Leveraging Large Models for Robot Learning

Research on large models, typically Large Language Models (LLMs) [28] and Visual Language Models (VLMs) [8], [29], [30], [27], has grown rapidly in recent years. Inspired by this, RT-1 [31] and RT-2 [32] explore the training of large models using large-scale demonstrations for robotic manipulation tasks. However, this necessitates a challenging data collection process that takes years to complete.

As a result, the robotics community has started to integrate the pre-trained large models into the robot learning workflow [33], [34], [35], [36], [37], [38], [7], [24], [25], [26]. In navigation, VLMs [33] and NavGPT [34] leverage the LLM to translate natural language instructions into explicit goals or actions. In manipulation, SayCan [38] leverages VLM to generate proposals for a given demand. Code-as-Policies [37] and Text2motion [36] leverage LLM to generate high-level plans for long-horizon tasks. VoxPoser [35] employs VLM and LLM collaboratively to synthesize robot trajectories. In rearrangement, DalleBot [7], TidyBot [26], [24] and [25] leverages VLM or LLM for goal specification.

Different from integration-based methods, we explore a distillation-based approach that extracts the functional rearrangement priors from the large models. A concurrent work [39] also distilled robot skills from LLM. Differently, we simultaneously distilled knowledge from both LLM and VLM, rather than just VLM, and we distilled more fine-grained (*i.e.*, coordinate-level) functional rearrangement priors.

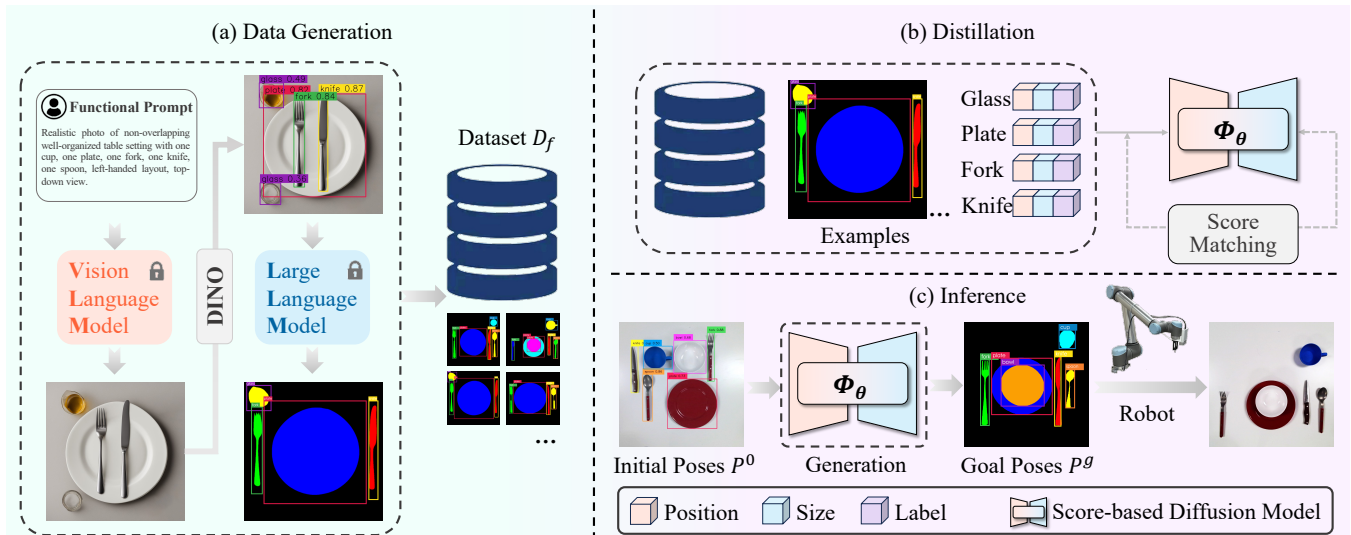


Fig. 2. **(a) Data Generation:** We construct an autonomous data collection pipeline to obtain arrangement examples, denoted as $D_f = \{(P^i, C^i)\}_{i=1}^K$, in two stages, collaboratively using an LLM and a VLM. First, we generate initial arrangement examples, $\{(\hat{P}^i, \hat{C}^i)\}_{i=1}^K$, by prompting the VLM and extracting object positions via GroundingDino. Then, we refine these examples using the LLM to obtain the final dataset, D_f . **(b) Distillation:** The collected dataset is distilled into a score-based diffusion model, denoted as Φ_θ , using a score-matching objective. **(c) Inference:** During test time, we generate goal positions, P^g , using the learned diffusion model and rearrange objects from the initial positions, P^0 , to the goal positions, P^g .

III. METHOD

Task Description: We aim to rearrange objects to meet functional requirements on a 2D planar surface, such as a dinner table, etc. In formal terms, we denote the functional requirements, such as "set up the dinner table for a left-handed person," as f . The AI robot is provided with a visual observation $I_O \in \mathbb{R}^{3 \times H \times W}$ of the scene from a top-down view. Assuming there are N objects denoted as $O = [o_1, o_2, \dots, o_N]$, the objective of the AI robot is to specify a set of target poses $P^g = [p_1^g, p_2^g, \dots, p_N^g]$ and move the objects from their initial poses $P^0 = [p_1^0, p_2^0, \dots, p_N^0]$ to target poses P^g .

Ideally, both the initial and goal poses should include 2D positions and 1D rotations, i.e., $p_i^0, p_i^g \in \text{SE}(2)$. However, in this work, we only consider the 2D position, i.e., $p_i^0, p_i^g \in \mathbb{R}^2$, since the existing RGB-based 2D pose estimation does not support a sufficient number of object categories.

Overview: Our goal is to train a conditional generative model capable of generating rearrangement goals compatible with the initial object conditions. Initially, we collect a dataset (Sec. III-A) using a Language Model (LLM) and a Vision Language Model (VLM), denoted as $D_f = \{(P^i, C^i) \sim p_f(P, C)\}_{i=1}^K$, where p_f represents the data distribution of D_f . Here, $C = [c_1, c_2, \dots, c_N]$, with $c_i = [s_i, y_i]$, describing the condition of the i -th object o_i . Specifically, $s_i \in \mathbb{R}^2$ denotes the object's 2-D axis-aligned bounding box dimensions, and $y_i \in \mathbb{R}^1$ is its category label. Then, we train a score-based diffusion model (Sec. III-B), referred to as Φ_θ , to model the conditional distribution $p_f(P|C)$ using the distilled dataset.

During inference (Sec. III-C), we start by computing the initial object conditions C from the visual observation I_O . Next, we generate a feasible goal P^g conditioned on the initial object configurations C using the trained diffusion model Φ_θ , and finally, we create a plan to achieve this goal.

A. Collaboratively Collecting Data through LLM and VLM

To extract functional rearrangement prior knowledge from large models, we construct an autonomous data collection pipeline to obtain the arrangement examples $D_f = \{(P^i, C^i) \sim p_f(P, C)\}_{i=1}^K$. This approach allows us to generate a large number of arrangement examples without the need for human labor across various configurations. To achieve this, we sample arrangement examples in two stages, collaboratively using LLM and VLM: we first generate initial arrangement examples $\{(\hat{P}^i, \hat{C}^i)\}_{i=1}^K$ using VLM and then refine these examples using LLM to obtain the final examples D_f .

At the first stage, For each instance, we initially prompt the VLM (i.e., StableDiffusion XL [8]) to get an image. The prompt is constructed as follows:

Realistic photo of <adjective> <setting description> with <num1> <object1>, <num2> <object2>, ..., <functional layout>, <view point>.

Subsequently, we extract initial objects' positions \hat{P} and conditions \hat{C} from the image using a large vision model for object detection, i.e., GroundingDino [12]. However, we observed that the layouts generated by the VLM are generally incompatible with the input prompt. Therefore, we leverage GroundingDino to detect and filter out images with unexpected categories or excessive numbers (i.e., surpassing three) from the same category.

Then, we introduce the second stage to refine the initial arrangement examples $\{(\hat{P}^i, \hat{C}^i)\}_{i=1}^K$. The refinement procedure is decomposed into two critical phases through the implementation of the Chain-of-Thoughts (CoT) strategy. In the first phase, we initiate the LLM by presenting the task introduction, user information, and the descriptions of all items on the table including the bounding box and category, provided by the detection module. This process aims to generate detailed functional requirements for the

expected arrangements. Subsequently, we prompt the LLM to infer the types and quantities of objects necessary for the functional scene, delete the redundant items, and reposition the remaining objects to generate expected coordinate-level layouts, aligning with the established functional requirements in the first phase. To better regularize the output of the second phase, we employ an in-context learning approach which is widely used in Natural Language Processing. By presenting manually designed instances as learning material, the LLM establishes the refined layout information in a compact and uniform format, contributing to the construction of the dataset. We defer the detailed prompt description to Appendix V-A.

B. Distilling Collected Dataset into a Diffusion Model

We further distill the collected arrangement examples, denoted as D_f , into a conditional generative model, Φ_θ . Our goal is to model the conditional data distribution, $p_f(P|C)$, using the conditional generative model, Φ_θ . This model is capable of generating reasonable object poses, P , that are compatible with the conditions of the objects, C . Consequently, we can utilize the distilled conditional generative model, Φ_θ , for goal specification during testing.

We employ the score-based diffusion model [9] to estimate the conditional distribution $p_f(P|C)$. Specifically, we construct a continuous diffusion process $\{P(t)\}_{t=0}^1$ indexed by a time variable $t \in [0, 1]$ using the Variance-Exploding (VE) Stochastic Differential Equation (SDE) proposed by [40], where $P(0) \sim p_f(P|C)$. The time-indexed pose variable $P(t)$ is perturbed by the following SDE as t increases from 0 to 1:

$$dP = \sqrt{\frac{d[\sigma^2(t)]}{dt}} dw, \quad \sigma(t) = \sigma_{\min} \left(\frac{\sigma_{\max}}{\sigma_{\min}} \right)^t \quad (1)$$

where $\{w(t)\}_{t \in [0, 1]}$ is the standard Wiener process [9], $\sigma_{\min} = 0.01$ and $\sigma_{\max} = 50$ are hyper-parameters.

Let $p_t(P|C)$ denote the marginal distribution of $P(t)$. We aim to estimate the *score function* of the perturbed conditional distribution $\nabla_P \log p_t(P|C)$ for all t during training:

$$p_t(P(t)|C) = \int \mathcal{N}(P(t); P(0), \sigma^2(t)\mathbf{I}) \cdot p_0(P(0)|C) dP(0) \quad (2)$$

It should be noted that when $t = 0$, $p_0(P(0)|C) = p_f(P(0)|C)$, which is exactly the data distribution.

Thanks to the Denoising Score Matching (DSM) [23], we can obtain a guaranteed estimation of $\nabla_P p_t(P|C)$ by training a score network $\Phi_\theta: \mathbb{R}^{|\mathcal{O}|} \times \mathbb{R}^1 \times \mathbb{R}^{|\mathcal{C}|} \rightarrow \mathbb{R}^{|\mathcal{O}|}$ via the following objective $\mathcal{L}(\theta)$:

$$\mathbb{E}_{t \sim \mathcal{U}(\varepsilon, 1)} \left\{ \lambda(t) \mathbb{E} \left[\left\| \Phi_\theta(P(t), t|C) - \frac{P(0) - P(t)}{\sigma(t)^2} \right\|_2^2 \right] \right\} \quad (3)$$

where $P(0) \sim p_f(P(0)|C)$ and $P(t) \sim \mathcal{N}(P(t); P(0), \sigma^2(t)\mathbf{I})$. ε is a hyper-parameter that denotes the minimal noise level. When minimizes the objective in Eq. 3, the optimal score network satisfies $\Phi_\theta^*(P, t|C) = \nabla_P \log p_t(P|C)$ [23].

After training, we can approximately sample goal poses from $p_f(P|C)$ by sampling from $p_\varepsilon(P|C)$, as $\lim_{\varepsilon \rightarrow 0} p_\varepsilon(P|C) = p_f(P|C)$. Sampling from $p_\varepsilon(P|C)$ requires

solving the following *Probability Flow* (PF) ODE [40] where $P(1) \sim \mathcal{N}(\mathbf{0}, \sigma_{\max}^2 \mathbf{I})$, from $t = 1$ to $t = \varepsilon$:

$$\frac{dP}{dt} = -\sigma(t)\dot{\sigma}(t)\nabla_P \log p_t(P|C) \quad (4)$$

where the score function $\log p_t(P|C)$ is empirically approximated by the trained score network $\Phi_\theta(P, t|C)$ and the ODE trajectory is solved by RK45 ODE solver [41].

The score network $\Phi_\theta(P, t|C)$ is implemented as a graph neural network, so as to adapt to the varied number of input objects. We construct all the objects as a fully-connected graph where the i -th node contains the pose p_i (*i.e.*, 2-D position) and the condition c_i (*i.e.*, 2-D sizes and 1-D label) of the i -th object. The score network encodes the input graph by two layers of Edge-Convolution [42] layers and outputs the score components on each node. The time variable t is encoded into a vector by a commonly used projection layer following [40]. This vector is concatenated into intermediate features output by the Edge-Convolution layers. We defer full training and architecture details to Appendix V-C.

C. Rearrange Objects with the Trained Diffusion Model

During test time, we first extract initial objects' conditions C and poses P^0 from the visual observation I_O via GroundingDino. We then generate goal poses P^g for the objects with the trained score network Φ_θ via Eq. 4.

To reach the goal, we first reorder the object list by prompting GPT4 to ensure that the containers (*e.g.*, saucers) will be rearranged before 'non-containers' (*e.g.*, mugs):

$$o_j \text{ is a container while } o_i \text{ is not} \Rightarrow o_i \succ o_j \quad (5)$$

Then we calculate the picking and placing points for each object using SuctionNet [43] and execute the pick-place actions. The detailed procedure is summarized below:

Algorithm 1 Test Time Rearrangement Algorithm

- 1: **Initialization:** Learned score network Φ_θ , number of objects N
 - 2: Receive visual observation I_O
 - 3: Extract initial object poses P^0 and conditions C from I_O
 - 4: Generate goal poses $P^g \sim p_f(P|C)$ using Eq. 4
 - 5: Reorder the object list $\{o_i\}$ according to
 - 6: **for** $i = 1$ **to** N **do**
 - 7: Compute translation \mathcal{T}_i for o_i according to p_i^0 and p_i^g
 - 8: **for** $j = i + 1$ **to** N **do**
 - 9: **if** o_i will collide with o_j after translation **then**
 - 10: Move o_j away
 - 11: **end if**
 - 12: **end for**
 - 13: Get the picking point p_{pick} by SuctionNet
 - 14: Get the placing point p_{place} according to p_{pick} and \mathcal{T}_i
 - 15: Execute picking p_{pick} and placing p_{place}
 - 16: **end for**
-

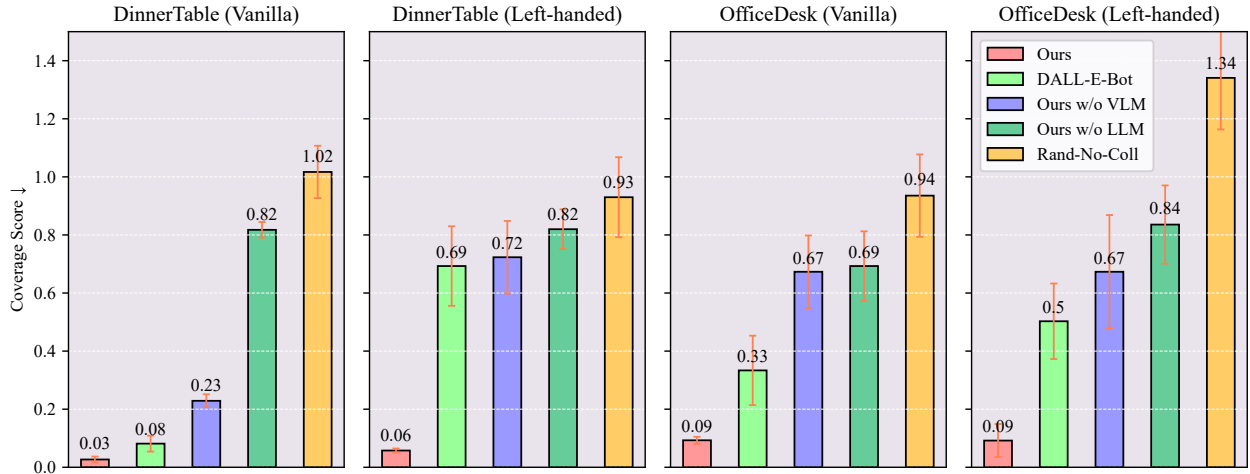


Fig. 3. Quantitative results across four domains, specifically Coverage Score bars for two functional settings (Vanilla and Left-handed) in two scenarios (Dinner table and Office desk). The mean and standard deviation are reported for comparison among our methods and baseline algorithms.

IV. EXPERIMENTS

Similar to [7], we evaluate our method using both subjective and objective metrics. In Sec IV-A, we will first introduce the domains and baselines used in our experiments. In Sec IV-B, we collect a test set that contains 30 ground truth arrangements for each domain and evaluate the effectiveness of each method in generating proper arrangements that satisfy different functional requirements under various configurations. In Sec IV-C, we conduct real-world rearrangement experiments at scale and measure the quality of the rearrangement results through user ratings. We defer the detailed experimental setups and implementation details to supplementary.

A. Setups

Domains. We consider four domains formed by the combination of two scenarios, namely, the dinner table and office desk, and two functionalities, which are “setting the table for right-handed people” (Vanilla) and “setting the table for left-handed people” (Left-handed). These domains are labeled as follows: *DinnerTable (Vanilla)*, *DinnerTable (Left-handed)*, *OfficeDesk (Vanilla)*, and *OfficeDesk (Left-handed)*. We generated 969, 132, 165, and 161 examples, respectively, for the four domains mentioned above using our autonomous data generation pipeline to train the diffusion model.

Baselines. We compare our method with a zero-shot baseline called *DALL-E-Bot*, which integrates a VLM into the rearrangement pipeline without the need for a dataset that requires human annotation or designation. Following the approach in [7], we also compare our method with the *Rand-No-Coll* baseline, which randomly places objects in the environment while ensuring they do not overlap.

B. Arrangement Evaluation

In the following experiments, we focus on evaluating the effectiveness in generating proper arrangement goals and do not consider the rearrangement process. For all the methods, we generate arrangements for the 30 test set configurations from each domain. In the case of *DALL-E-Bot*, we take the target poses after the ICP-matching as its arrangement results

since we do not provide an initial state. To evaluate the generated arrangement goals, we employ the *Coverage Score* proposed by [2], which measures the diversity and fidelity of the rearrangement results by calculating the Minimal-Matching-Distance (MMD) [44] between the P_{gen} and a fixed set of ground-truth examples P_{gt} from the test set:

$$\sum_{p_{gt} \in P_{gt}} \min_{p_{gen} \in P_{gen}} \|p_{gt} - p_{gen}\|_2^2. \quad (6)$$

As shown in Fig. 3, our method significantly outperforms all the baselines across four domains, showcasing the effectiveness of our method in generating arrangement goals. The lower-bound method, *Rand-No-Coll*, consistently achieves the worst performance, highlighting the effectiveness of the *Coverage Score* metric. Notably, in all the *Left-handed* domains, our method exhibits a greater advantage compared to *DALL-E-Bot* than *Vanilla*’s. This is because VLM struggles to align with the functional requirements in the prompt, whereas our approach, which refines VLM using LLM, ensures that the training data better aligns with the functional requirements.

TABLE I

ANALYZE THE MARGINAL KL-DIVERGENCE ON *DinnerTable (Left-handed)*.

	Plate2Fork ↓	Plate2Knife ↓	Plate2Spoon ↓
Rand-No-Coll	74.45	34.21	12.40
DALL-E-Bot	73.48	32.41	11.52
Ours	6.72	6.81	12.59
Ours w/o LLM	72.29	35.17	6.28
Ours w/o VLM	78.46	27.42	8.94

To gain an in-depth understanding of our advantages, we conduct further marginal statistical analysis on *DinnerTable (Left-handed)*. Specifically, we introduce *marginal-KL-analysis*, which calculates the relative positional distribution of two specific categories (e.g., Plate2Fork) of items within the results generated by various methods and determines the KL-distance between this distribution and the one observed in the test dataset. Detailed information about this metric is deferred to Appendix V-B.

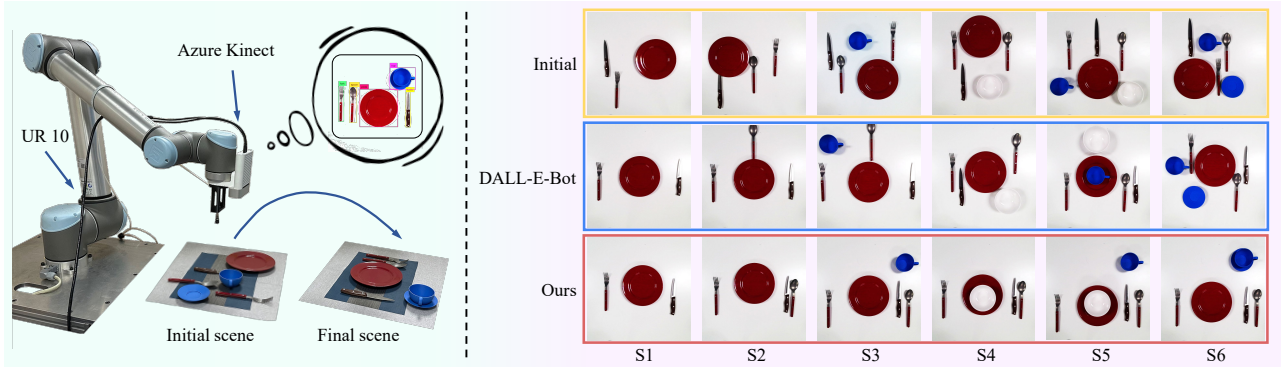


Fig. 4. **Left:** The real-world setup for object rearrangement. **Right:** Qualitative results of real-world experiments on *DinnerTable (Vanilla)*. We design 6 different scenes (i.e., $S1 \sim S6$) with increasing complexity.

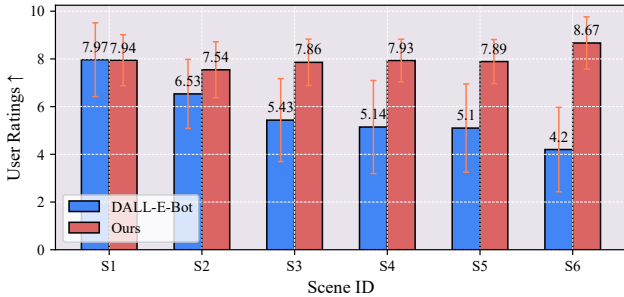


Fig. 5. User ratings for each method on real-world arrangements. Each bar demonstrates the mean and standard deviation across all users.

As shown in Table I, our method outperforms the baselines in most cases. In *Plate2Spoon*, our method still achieves comparable performance to the *DALL-E-Bot*.

Notably, both VLM and LLM play crucial roles in our method’s performance. As demonstrated in Fig.3 and Table I, our method experiences a significant performance drop when either LLM or VLM is ablated, to the extent that it falls significantly below *DALL-E-Bot*.

C. Real World Rearrangement Experiments

In the following experiments, we focus on evaluating the effectiveness of our method in real-world rearrangement. We compare our method with the most competitive baseline, *DALL-E-Bot*, as verified in objective evaluations (see Section IV-B). To ensure a fair comparison, we designed 6 different scenes (denoted as $S1 \sim S6$, the scene complexity increase from $S1$ to $S6$) with 3 different initializations within *DinnerTable (Vanilla)* domain and deployed both methods on the same set of initial configurations. As depicted in Fig.4 (a), the real-world experiments were conducted using a UR10 robot arm equipped with an Azure Kinect RGBD camera. Similar to the approach in[7], we conducted a user study to evaluate the rearrangement results, as there are no ground truth arrangements in the real-world setting. The user is asked to provide a score from 1 (very bad) to 10 (very good), according to their preferences and functional requirements. We recruited 30 users, including both male and female, with ages ranging from 18 to 55. Each rearrangement result is assessed by all the users, resulting in a total of 900 ratings.

As depicted in Fig. 4 (b), as the complexity of the scene

TABLE II
MODEL PARAMETERS

	Ours	StableDiffusion XL
Number of Parameters↓	180K	3.5B

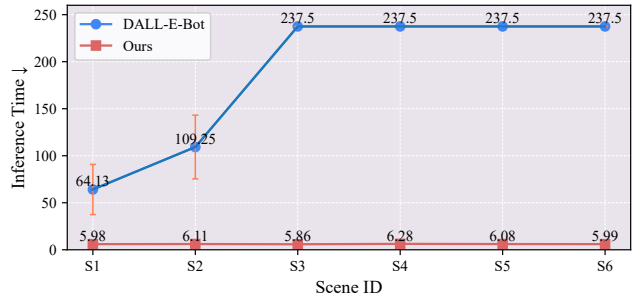


Fig. 6. **Inference time** for each method on real-world arrangements. The complexity of the scene gradually increases from $S1$ to $S6$.

increases, *DALL-E-Bot* experiences a decline in performance, whereas our approach’s performance remains stable. The results presented in Fig. 5 consistently demonstrate this phenomenon: the average user rating for *DALL-E-Bot* decreases from $S1$ to $S6$, whereas our method not only maintains its performance but also exhibits slight improvement. These findings highlight the effectiveness of our approach in generating compatible and robust goals for object rearrangement.

Finally, our approach boasts greater time efficiency because we distill knowledge from the large model (3.5B parameters for StableDiffusion XL) into a lightweight compact representation (180K parameters for ours), avoiding repeated inference of the large model at test time. To illustrate this point, we conducted an evaluation of the average inference times required for goal specification in our method as compared to *DALL-E-Bot* on the *DinnerTable (Vanilla)* dataset, using 10 identical initializations. As detailed in Fig. 6, our method achieves a substantial advantage in terms of efficiency. This advantage arises because VLM-generated images often struggle to pass the filter when dealing with complex scenes. In the context of $S3$ - $S6$, marked by higher complexity, *DALL-E-Bot* consistently fails to pass the filter and surpasses the designated filtration budget (≤ 10), resulting in the same long inference time. In contrast, our method consistently generates compatible layouts in a few seconds.

V. CONCLUSION

We are the first to distill functional rearrangement priors from large models for object rearrangement tasks. Specifically, we propose a novel approach that collects diverse arrangement examples using both LLMs and VLMs, and then distills the examples into a diffusion model. This approach leverages the scalability and generalization of large models to facilitate the distilled diffusion model in generating goals compatible with the initial configuration, effectively addressing compatibility issues. Our results, including real-world experiments, significantly outperform baselines quantitatively and qualitatively. Furthermore, our further analysis suggests that both VLM and LLM play crucial roles in the performance of our method.

Future work could involve implementing rotation-aware perception and incorporating language conditions to further enhance the performance and capabilities of our method.

REFERENCES

- [1] D. Batra, A. X. Chang, S. Chernova, A. J. Davison, J. Deng, V. Koltun, S. Levine, J. Malik, I. Mordatch, R. Mottaghi *et al.*, “Rearrangement: A challenge for embodied ai,” *arXiv preprint arXiv:2011.01975*, 2020.
- [2] M. Wu, F. Zhong, Y. Xia, and H. Dong, “TarGF: Learning target gradient field for object rearrangement,” *arXiv preprint arXiv:2209.00853*, 2022.
- [3] Y. Shen, Y. Tay, C. Zheng, D. Bahri, D. Metzler, and A. Courville, “Structformer: Joint unsupervised induction of dependency and constituency structure from masked language modeling,” *arXiv preprint arXiv:2012.00857*, 2020.
- [4] W. Liu, T. Hermans, S. Chernova, and C. Paxton, “Structdiffusion: Object-centric diffusion for semantic rearrangement of novel objects,” *arXiv preprint arXiv:2211.04604*, 2022.
- [5] A. Simeonov, A. Goyal, L. Manuelli, L. Yen-Chen, A. Sarmiento, A. Rodriguez, P. Agrawal, and D. Fox, “Shelving, stacking, hanging: Relational pose diffusion for multi-modal rearrangement,” *arXiv preprint arXiv:2307.04751*, 2023.
- [6] I. Kapelyukh and E. Johns, “My house, my rules: Learning tidying preferences with graph neural networks,” in *5th Annual Conference on Robot Learning*, 2021.
- [7] I. Kapelyukh, V. Vosylius, and E. Johns, “Dall-e-bot: Introducing web-scale diffusion models to robotics,” *IEEE Robotics and Automation Letters*, 2023.
- [8] R. Rombach, A. Blattmann, D. Lorenz, P. Esser, and B. Ommer, “High-resolution image synthesis with latent diffusion models,” in *Proceedings of the IEEE/CVF conference on computer vision and pattern recognition*, 2022, pp. 10 684–10 695.
- [9] Y. Song, J. Sohl-Dickstein, D. P. Kingma, A. Kumar, S. Ermon, and B. Poole, “Score-based generative modeling through stochastic differential equations,” in *International Conference on Learning Representations*, 2021. [Online]. Available: <https://openreview.net/forum?id=PxtTIG12RRHS>
- [10] K. Lee, H. Liu, M. Ryu, O. Watkins, Y. Du, C. Boutilier, P. Abbeel, M. Ghavamzadeh, and S. S. Gu, “Aligning text-to-image models using human feedback,” *arXiv preprint arXiv:2302.12192*, 2023.
- [11] K. Black, M. Janner, Y. Du, I. Kostrikov, and S. Levine, “Training diffusion models with reinforcement learning,” *arXiv preprint arXiv:2305.13301*, 2023.
- [12] S. Liu, Z. Zeng, T. Ren, F. Li, H. Zhang, J. Yang, C. Li, J. Yang, H. Su, J. Zhu *et al.*, “Grounding dino: Marrying dino with grounded pre-training for open-set object detection,” *arXiv preprint arXiv:2303.05499*, 2023.
- [13] J. Wei, X. Wang, D. Schuurmans, M. Bosma, F. Xia, E. Chi, Q. V. Le, D. Zhou *et al.*, “Chain-of-thought prompting elicits reasoning in large language models,” *Advances in Neural Information Processing Systems*, vol. 35, pp. 24 824–24 837, 2022.
- [14] N. Abdo, C. Stachniss, L. Spinello, and W. Burgard, “Robot, organize my shelves! tidying up objects by predicting user preferences,” in *2015 IEEE International Conference on Robotics and Automation (ICRA)*. IEEE, 2015, pp. 1557–1564.
- [15] M. J. Schuster, D. Jain, M. Tenorth, and M. Beetz, “Learning organizational principles in human environments,” in *2012 IEEE International Conference on Robotics and Automation*. IEEE, 2012, pp. 3867–3874.
- [16] N. Abdo, C. Stachniss, L. Spinello, and W. Burgard, “Organizing objects by predicting user preferences through collaborative filtering,” *The International Journal of Robotics Research*, vol. 35, no. 13, pp. 1587–1608, 2016.
- [17] M. Fisher, D. Ritchie, M. Savva, T. Funkhouser, and P. Hanrahan, “Example-based synthesis of 3d object arrangements,” *ACM Transactions on Graphics (TOG)*, vol. 31, no. 6, pp. 1–11, 2012.
- [18] L. F. Yu, S. K. Yeung, C. K. Tang, D. Terzopoulos, T. F. Chan, and S. J. Osher, “Make it home: automatic optimization of furniture arrangement,” *ACM Transactions on Graphics (TOG)-Proceedings of ACM SIGGRAPH 2011*, v. 30,(4), July 2011, article no. 86, vol. 30, no. 4, 2011.
- [19] Y.-T. Yeh, L. Yang, M. Watson, N. D. Goodman, and P. Hanrahan, “Synthesizing open worlds with constraints using locally annealed reversible jump mcmc,” *ACM Transactions on Graphics (TOG)*, vol. 31, no. 4, pp. 1–11, 2012.
- [20] A. Handa, V. Patrăucean, S. Stent, and R. Cipolla, “Scenet: An annotated model generator for indoor scene understanding,” in *2016 IEEE International Conference on Robotics and Automation (ICRA)*. IEEE, 2016, pp. 5737–5743.
- [21] S. Qi, Y. Zhu, S. Huang, C. Jiang, and S.-C. Zhu, “Human-centric indoor scene synthesis using stochastic grammar,” in *Proceedings of the IEEE Conference on Computer Vision and Pattern Recognition*, 2018, pp. 5899–5908.
- [22] Q. A. Wei, S. Ding, J. J. Park, R. Sajjani, A. Poulenard, S. Sridhar, and L. Guibas, “Lego-net: Learning regular rearrangements of objects in rooms,” in *Proceedings of the IEEE/CVF Conference on Computer Vision and Pattern Recognition*, 2023, pp. 19 037–19 047.
- [23] P. Vincent, “A connection between score matching and denoising autoencoders,” *Neural Computation*, vol. 23, no. 7, pp. 1661–1674, 2011.
- [24] Y. Kant, A. Ramachandran, S. Yenamandra, I. Gilitschenski, D. Batra, A. Szot, and H. Agrawal, “Housekeep: Tidying virtual households using commonsense reasoning,” *arXiv preprint arXiv:2205.10712*, 2022.
- [25] G. Sarch, Z. Fang, A. W. Harley, P. Schydlow, M. J. Tarr, S. Gupta, and K. Fragkiadaki, “Tidee: Tidying up novel rooms using visuo-semantic commonsense priors,” *arXiv preprint arXiv:2207.10761*, 2022.
- [26] J. Wu, R. Antonova, A. Kan, M. Lepert, A. Zeng, S. Song, J. Bohg, S. Rusinkiewicz, and T. Funkhouser, “Tidybot: Personalized robot assistance with large language models,” *arXiv preprint arXiv:2305.05658*, 2023.
- [27] A. Ramesh, P. Dhariwal, A. Nichol, C. Chu, and M. Chen, “Hierarchical text-conditional image generation with clip latents,” *arXiv preprint arXiv:2204.06125*, vol. 1, no. 2, p. 3, 2022.
- [28] OpenAI, “Gpt-4 technical report,” *ArXiv*, vol. abs/2303.08774, 2023.
- [29] A. Radford, J. W. Kim, C. Hallacy, A. Ramesh, G. Goh, S. Agarwal, G. Sastry, A. Askell, P. Mishkin, J. Clark *et al.*, “Learning transferable visual models from natural language supervision,” in *International conference on machine learning*. PMLR, 2021, pp. 8748–8763.
- [30] D. Driess, F. Xia, M. S. Sajjadi, C. Lynch, A. Chowdhery, B. Ichter, A. Wahid, J. Tompson, Q. Vuong, T. Yu *et al.*, “Palm-e: An embodied multimodal language model,” *arXiv preprint arXiv:2303.03378*, 2023.
- [31] A. Brohan, N. Brown, J. Carbajal, Y. Chebotar, J. Dabis, C. Finn, K. Gopalakrishnan, K. Hausman, A. Herzog, J. Hsu *et al.*, “Rt-1: Robotics transformer for real-world control at scale,” *arXiv preprint arXiv:2212.06817*, 2022.
- [32] B. Zitkovich, T. Yu, S. Xu, P. Xu, T. Xiao, F. Xia, J. Wu, P. Wohlhart, S. Welker, A. Wahid *et al.*, “Rt-2: Vision-language-action models transfer web knowledge to robotic control,” in *7th Annual Conference on Robot Learning*, 2023.
- [33] C. Huang, O. Mees, A. Zeng, and W. Burgard, “Visual language maps for robot navigation,” in *2023 IEEE International Conference on Robotics and Automation (ICRA)*. IEEE, 2023, pp. 10 608–10 615.
- [34] G. Zhou, Y. Hong, and Q. Wu, “Navgpt: Explicit reasoning in vision-and-language navigation with large language models,” *arXiv preprint arXiv:2305.16986*, 2023.
- [35] W. Huang, C. Wang, R. Zhang, Y. Li, J. Wu, and L. Fei-Fei, “Voxposer: Composable 3d value maps for robotic manipulation with language models,” *arXiv preprint arXiv:2307.05973*, 2023.
- [36] K. Lin, C. Agia, T. Migimatsu, M. Pavone, and J. Bohg, “Text2motion:

From natural language instructions to feasible plans,” *arXiv preprint arXiv:2303.12153*, 2023.

- [37] J. Liang, W. Huang, F. Xia, P. Xu, K. Hausman, B. Ichter, P. Florence, and A. Zeng, “Code as policies: Language model programs for embodied control,” in *2023 IEEE International Conference on Robotics and Automation (ICRA)*. IEEE, 2023, pp. 9493–9500.
- [38] M. Ahn, A. Brohan, N. Brown, Y. Chebotar, O. Cortes, B. David, C. Finn, C. Fu, K. Gopalakrishnan, K. Hausman *et al.*, “Do as i can, not as i say: Grounding language in robotic affordances,” *arXiv preprint arXiv:2204.01691*, 2022.
- [39] H. Ha, P. Florence, and S. Song, “Scaling up and distilling down: Language-guided robot skill acquisition,” *arXiv preprint arXiv:2307.14535*, 2023.
- [40] Y. Song, J. Sohl-Dickstein, D. P. Kingma, A. Kumar, S. Ermon, and B. Poole, “Score-based generative modeling through stochastic differential equations,” *arXiv preprint arXiv:2011.13456*, 2020.
- [41] J. R. Dormand and P. J. Prince, “A family of embedded runge-kutta formulae,” *Journal of computational and applied mathematics*, vol. 6, no. 1, pp. 19–26, 1980.
- [42] X. Zhang, C. Xu, X. Tian, and D. Tao, “Graph edge convolutional neural networks for skeleton-based action recognition,” *IEEE transactions on neural networks and learning systems*, vol. 31, no. 8, pp. 3047–3060, 2019.
- [43] H. Cao, H.-S. Fang, W. Liu, and C. Lu, “Suctionnet-1billion: A large-scale benchmark for suction grasping,” *IEEE Robotics and Automation Letters*, vol. 6, no. 4, pp. 8718–8725, 2021.
- [44] P. Achlioptas, O. Diamanti, I. Mitliagkas, and L. Guibas, “Learning representations and generative models for 3d point clouds,” in *International Conference on Machine Learning*. PMLR, 2018, pp. 40–49.

APPENDIX

A. Prompt Engineering for LLM

Example for *Left-handed Dinner Table* scene:

Phase 1: Query LLM about functional requirements

User Input

Utilize your expertise in dining table arrangement and spatial reasoning to create an organized layout suitable for left-handed individuals. please instruct me on how to rearrange these items [plate, fork, knife, spoon, bowl, cup, mug]. Your response should be in list format, with each line not exceeding twenty words, and no additional information.

LLM Output

1. **Plate:** Center of the table.
2. **Fork:** Right of the plate.
3. **Knife:** Left of the plate, blade facing inward.
4. **Spoon:** Left of the knife.
5. **Bowl:** Above the plate, on the left side.
6. **Cup:** Above the spoon, to the left of the bowl.
7. **Mug:** To the left of the cup.

Phase 2: Prompt the LLM to infer the types and quantities of objects necessary for the functional scene, delete the redundant items, and reposition the remaining objects to generate the expected coordinate-level layouts, aligning with the established functional requirements in Phase 1.

User Input

The user will give you several bounding boxes of objects on a 1024*1024 image, the bounding box format is [xmin, ymin, xmax, ymax, label]. There are some objects you should remove. this dining table setting is only for one left-handed person.

Use the following step-by-step instructions to respond.

Step 1 - Depending on the number of dining people you infer, list how many of each item is needed

Step 2 - Depending on the number of each item you need, remove the bounding box that contains unnecessary items till the number of each item is consistent with the number you raised in Step 1.

Step 3 - After removing, you should move the remaining coordinate of the bounding box to achieve spatial reasoning and a well-organized dining table setting for left-handed people, and the size of the bounding box you removed should not change.

your answer should be brief. please follow below desired format below:

<Output Format>

Here is an example for in-context learning: <In Context Example>

where the *Output Format* and the *In Context Example* are shown below:

Output Format

Number to remove:
Number to move:
Rearrange bounding box:
Num of each object:
Rearrange bounding box:
From:
To:
Modified list:

In Context Example

User input:

[[892, 233, 939, 822, 'knife'], [944, 338, 1023, 817, 'spoon'], [48, 276, 121, 828, 'fork'], [111, 107, 903, 853, 'plate'], [838, 1, 994, 177, 'glass'], [265, 259, 842, 734, 'bowl']]

Output:

Number to move: 5 (Plate, Knife, Spoon, Fork, and Glass)

Rearrange Bounding Box:

Plate: From: [111, 107, 903, 853] To: [111, 107, 903, 853] (No change in size and position)

Knife: From: [892, 233, 939, 822] To: [60, 233, 107, 822] (Moved to the left side of the plate)

Spoon: From: [944, 338, 1023, 817] To: [8, 338, 87, 817] (Moved to the far left, to the left of the knife, not overlap a lot with a knife)

Fork: From: [48, 276, 121, 828] To: [903, 276, 976, 828] (Moved to the right side of the plate)

Glass: From: [838, 1, 994, 177] To: [600, 1, 756, 177] (Moved above the plate, at a centralized position)

Bowl: Unchanged: [265, 259, 842, 734]

Modified List: [[60, 233, 107, 822, 'knife'], [8, 338, 87, 817, 'spoon'], [903, 276, 976, 828, 'fork'], [111, 107, 903, 853, 'plate'], [600, 1, 756, 177, 'glass'], [265, 259, 842, 734, 'bowl']]

LLM Output

To assist with your dining table rearrangement task for a left-handed person, I will need the bounding box coordinates and labels of the items on the table. Once you provide these details, I can guide you through the steps to organize the items according to the requirements you've outlined. Please share the bounding box information for the items on your dining table.

Phase 3: Continuously corrected data generation. After initiating the LLM following the aforementioned two phases above, it can leverage its general knowledge and logical reasoning skills to consistently rectify the initial layouts gen-

erated by the VLM, and provide well-formulated descriptions for each corrected layout thanks to in-context learning.

Extrated Information From VLM Output

[[837, 98, 918, 955, 'knife'], [370, 148, 462, 950, 'fork'], [131, 77, 854, 819, 'plate'], [457, 155, 590, 841, 'spoon'], [74, 704, 260, 887, 'cup']]

LLM Output

Modified list: [[75, 98, 156, 955, 'knife'], [10, 155, 143, 841, 'spoon'], [855, 148, 947, 950, 'fork'], [131, 77, 854, 819, 'plate'], [600, 704, 786, 887, 'cup']]

The LLM outputs from each scene will serve as the foundation for constructing our dataset.

B. Details of Marginal KL-divergence Analysis

Marginal KL-Divergence is employed to assess the relative 2D positional distribution of two specific categories. Initially, we performed the following 2D Gaussian Kernel Density Estimation (KDE) function to estimate the probability density of 2D positional distances between the two categories:

$$\hat{f}(x,y) = \frac{1}{nh_xh_y} \sum_{i=1}^n K\left(\frac{x-x_i}{h_x}\right) \cdot K\left(\frac{y-y_i}{h_y}\right), \quad (7)$$

where (x,y) is the 2D relational distance of two points, n is the number of samples, h_x and h_y are bandwidth parameters in the x and y directions, respectively, and $K(u) = \frac{1}{\sqrt{2\pi}} e^{-\frac{u^2}{2}}$ is the kernel function, chosen as the probability density function of the standard normal distribution. Subsequently, we employed the following Kullback-Leibler Divergence (KLD) to measure the difference between the two probability distributions:

$$D_{KL}(P\|Q) = \sum_i P(i) \cdot \log\left(\frac{P(i)}{Q(i)}\right), \quad (8)$$

where event i represents data points of 2D positional distances between two specific categories, $P(i)$ and $Q(i)$ denote the probabilities of event i , computed from Eq. 7.

C. Training and Architectural Details of the Score Network

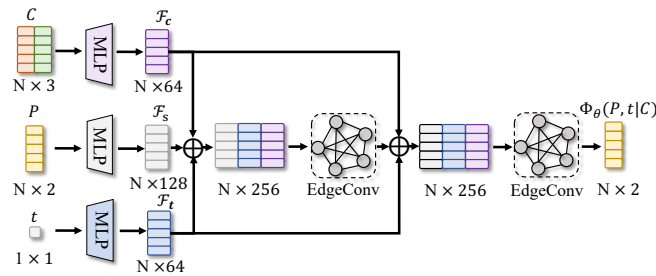


Fig. 7. Architecture of the Score Network

Training Details: We use the Adam optimizer with a learning rate of $2e-4$ for training, and the batch size is set to

16. It takes 9 hours to train on a single RTX 3090 for primitive policy to converge. The number of steps ϵ is configured to 500 in the sampling process.